



ALMA MATER STUDIORUM  
UNIVERSITÀ DI BOLOGNA

ARCHIVIO ISTITUZIONALE  
DELLA RICERCA

## Alma Mater Studiorum Università di Bologna Archivio istituzionale della ricerca

Optimization of Corona Triode Polarization by 2D Electrostatic Mapping

This is the final peer-reviewed author's accepted manuscript (postprint) of the following publication:

*Published Version:*

L Gasperini, A.R. (2023). Optimization of Corona Triode Polarization by 2D Electrostatic Mapping. Piscataway, NJ : IEEE [10.1109/CEIDP51414.2023.10410529].

*Availability:*

This version is available at: <https://hdl.handle.net/11585/957482> since: 2024-02-13

*Published:*

DOI: <http://doi.org/10.1109/CEIDP51414.2023.10410529>

*Terms of use:*

Some rights reserved. The terms and conditions for the reuse of this version of the manuscript are specified in the publishing policy. For all terms of use and more information see the publisher's website.

This item was downloaded from IRIS Università di Bologna (<https://cris.unibo.it/>).  
When citing, please refer to the published version.

(Article begins on next page)

# Optimization of Corona Triode Polarization by 2D Electrostatic Mapping

L. Gasperini, A. Rumi, G. Selleri, D. Fabiani, P. Seri  
LIMES - Department of Electrical, Electronic and Information Engineering (DEI)  
University of Bologna, Bologna Italy

**Abstract-** Traditional methods for characterizing piezoelectric materials typically involve analyzing their electromechanical response, focusing on coefficients such as the piezoelectric strain coefficient  $d_{33}$ . In this study, an alternative approach is proposed to evaluate the piezoelectric response by examining the surface charge accumulated in the tested sample following a corona polarization process. Through the use of an electrostatic voltmeter, two influential factors affecting the piezoelectric response were investigated: the number of needles employed during the polarization and the presence of a grid interposed between the high-voltage needles and the specimen.

## I. INTRODUCTION

Piezoelectric polymeric materials have garnered significant attention and sparked widespread interest in recent years due to their remarkable properties and numerous potential applications. These materials, composed of polymers with intrinsic piezoelectric characteristics, exhibit the unique ability to convert mechanical stimuli into electrical signals. This property has led to their utilization in various fields, including the development of sensors, such as pressure or acoustic sensors, and the creation of flexible wearable energy harvesting devices.

The key phenomenon behind the functionality of piezoelectric polymeric materials is the piezoelectric effect. When subjected to mechanical stress or vibration, these materials generate electrical charges. This effect arises from the alignment of molecular dipoles within the crystalline lattice of the polymer, resulting in the separation of positive and negative charges and the generation of an electric field. By integrating piezoelectric materials into a hosting matrix, it becomes possible to create self-sensing composite materials capable of converting mechanical stimuli into measurable electrical signals [1], [2]. Furthermore, piezoelectric polymeric materials offer an attractive solution for harvesting ambient vibrations and mechanical movements to generate electricity. This characteristic presents an efficient and sustainable method for powering small-scale electronic devices, as these materials can scavenge and convert the surrounding mechanical energy into usable electrical energy [3], [4].

To confer a macroscale piezoelectric behavior to the polymeric materials and align the molecular dipoles within the crystalline lattice uniformly, a process called poling is required. Traditional polarization methods involve contact poling using direct or alternating current [5], [6]. However, these techniques often pose challenges, particularly when dealing with materials that require high coercive electric fields. Electrical breakdown

across the sample can occur, limiting the effectiveness of these conventional poling techniques.

In response to these challenges, alternative poling techniques have been developed to overcome the limitations of traditional methods. One such technique is corona poling, which operates on a non-contact principle. When a high voltage is applied, corona poling ionizes the air surrounding a metallic needle, creating a charged environment [7]. By placing the piezoelectric sample on a grounded plate, the generated ions flow from the needle towards the ground and deposit onto the surface of the sample, inducing the desired polarization [8], [9]. However, achieving uniform charge distribution over the sample surface remains a significant challenge in corona poling. To address the issue of non-uniform charge distribution, a significant advancement was made with the introduction of the corona triode technique. This technique involves the incorporation of a metallic grid connected to a high voltage generator between the needle and the sample. The addition of the grid enhances the uniformity of the charge distribution, improving the effectiveness of the corona poling process.

The corona poling process is influenced by various parameters, including the distances between the grid and ground, the needle and ground, the voltage values applied to the needles and grid, the temperature during poling, the duration of the poling process, and the number of needles used. Evaluating the impact of these parameters on the effectiveness of the polarization technique traditionally involves examining the piezoelectric strain coefficient,  $d_{33}$ , through electromechanical characterization. However, due to the potential non-uniform distribution of  $d_{33}$ , these measurements are typically conducted at multiple points, and the electrode used for characterization is often smaller in size compared to the sample.

In this study, the aim is to enable a rapid and comprehensive evaluation of the induced polarization in piezoelectric materials by employing surface potential mappings. This approach allows for the visualization and analysis of the charge distribution on the sample surface. The effectiveness of the corona poling process and the uniformity of the induced polarization can be evaluated more efficiently using this method [10]. Previous research has utilized surface potential mappings to explore the limits of charge uniformity achieved when using a tri-needle corona electrode on various dielectric materials. Additionally, the study investigates the effect of temperature control during corona poling on surface charge accumulation in polyimide (PI) films, using an electrostatic voltmeter to measure the surface potential [11], [12].

In this paper, thin films of polymeric polyvinylidene fluoride-trifluoroethylene (P(VDF-TrFE)) 80/20 are employed as the piezoelectric materials for the evaluation of induced polarization after the corona poling process. The assessment is facilitated by a custom-built 3-axis motorized stage combined with a non-contact probe of an electrostatic voltmeter. These experimental setups enable precise measurements and characterization of the polarization behavior in the P(VDF-TrFE) films, providing valuable insights into the effectiveness of corona poling and its potential applications in the field of piezoelectric materials.

## II. MATERIALS AND METHODS

Commercial P(VDF-TrFE) films were provided by Solvay S.p.A. Milan in A4 format and then shaped in smaller specimens (40 x 40 x 0.02 mm) on which the following test were carried out. A corona poling process (described in section A) was performed to polarize the specimens and the electrical charge distribution on the surface of the samples was mapped through a non-contact probe connected to an electrostatic voltmeter. Finally, an electromechanical characterization was performed to compare the piezoelectric strain coefficient  $d_{33}$  with the 2D electrostatic maps obtained.

### A. Corona Poling Process

Two types of corona poling process were implemented for the study of the surface charge accumulation on the P(VDF-TrFE) films: the gridless and the triode corona poling. The gridless corona poling consists of a needle holder connected to a high voltage generator (Fug HCN 35kV) and a grounded aluminum base where the specimen is placed. A polytetrafluoroethylene (PTFE) structure was employed to provide electrical insulation, thus separating the high-voltage electrode from the ground plate. The needle holder was attached to a brass rod, allowing the distance between the needle and the sample to be adjusted for different poling conditions. The polarization process took place at room temperature for 60 minutes at a distance of 40 mm between the needles and the ground plate, following the procedure already described in [13]. Three different tests were performed by varying the number of needles (1, 9 and 25) and by applying the same high voltage condition of 20 kV.

In the corona triode polarization process a metallic grid was interposed between the needle and the grounded base (Fig. 1). The grid was connected to a DC high voltage generator (Glassman High Voltage) set at 3 kV, with the purpose to ensure a more uniform distribution of ions on the sample surface. The distance between the needles and the grid was set at 35 mm, while the distance between the grid and the ground plate was set at 5 mm, maintaining a constant total distance of 40 mm, as in the gridless polarization process. In Table I the different specifications used for the experimental campaign are reported.

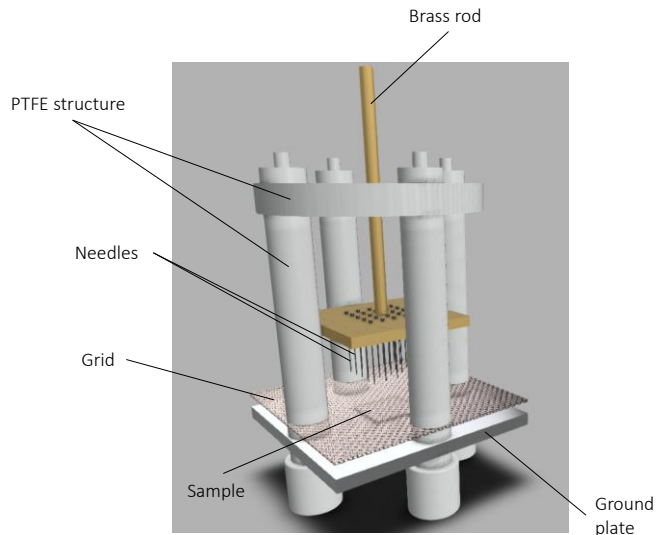


Fig. 1. Corona triode cell

TABLE I  
CORONA POLING TEST

Gridless Configuration		Corona Triode Configuration	
Specimen	Number of Needles	Specimen	Number of Needles
1	1	4	1
2	9	5	9
3	25	6	25

### B. Surface Potential Mapping Setup

To assess the uniformity of electrical charge distribution on the surface of the samples, a non-contact probe (TREK, model 3455ET) connected to a 20-kV electrostatic voltmeter (TREK, model 341B) was used to map the electrostatic potential on the specimen surfaces.

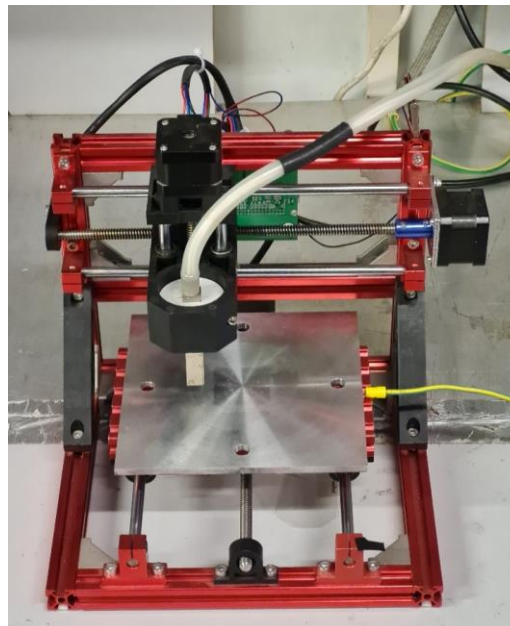


Fig. 2. 3-axis motorized stage used for the movement of the electrostatic probe

The probe was mounted on a custom made 3-axis motorized positioning stage (Fig. 2) with resolution of 0.1 mm, fixing the gap between the sensing element of the probe and the specimen to 5 mm. Specimens were fixed to a ground plane below the probe, and mapping was achieved monitoring the potential while following a predefined movement pattern (Fig. 3) at constant speed over the surface of the polarized specimen and reconstructing the 2D map in post processing. The whole process requires about 30 seconds to scan a 40x40 mm square sample.

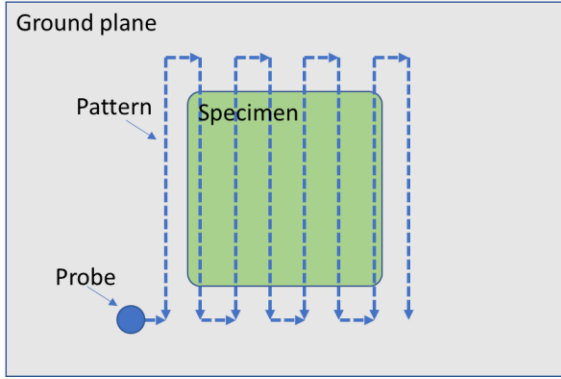


Fig. 3. Example of pattern followed by the probe over time at constant speed

### C. Electromechanical Characterization

Prior to conducting electromechanical tests, both surfaces of the polymeric film were grounded for 24 hours at room temperature. This step aimed to eliminate any residual electrostatic charges that might have been generated during the poling processes. The measurement of the piezoelectric strain

coefficient  $d_{33}$  (pC/N) for all polarized samples was performed using a piezometer (PiezoMeter PM300, Piezotest, Singapore, www.piezotest.com). The  $d_{33}$  value represents the ratio between the collected charge (Q) generated on the two opposite surfaces of the nanofibrous mats and the applied force (F), as defined in the following equation:

$$d_{33} = Q/F \quad [pC/N] \quad (1)$$

In order to measure the  $d_{33}$ , each sample was placed between two electrodes and secured with a screw clamp. The specimens were subjected to a compressive sinusoidal force oscillating between 0.25 N and 0.5 N at a frequency of 110 Hz. Since the electrodes of the piezometer had a smaller surface area than the P(VDF-TrFE) film, five different points on the sample surface were measured to thoroughly examine the uniformity of the piezoelectric response.

## III. RESULTS AND DISCUSSION

The electrical charge distribution on the piezoelectric sample after the corona poling process was evaluated through a non-contact probe combined with an electrostatic voltmeter. The ground base of the corona cell, where the specimen was placed, was removed and fixed below the probe immediately after the poling process (about 2 minutes). For each specimen a 2D map was obtained after the analysis of the surface potential and the six resulting maps were presented in Fig. 4. As can be observed (Fig. 4 from a) to c)), in the gridless corona poling process an increase in the number of needles led to a higher deposition of electric charges compared to the map obtained with only one

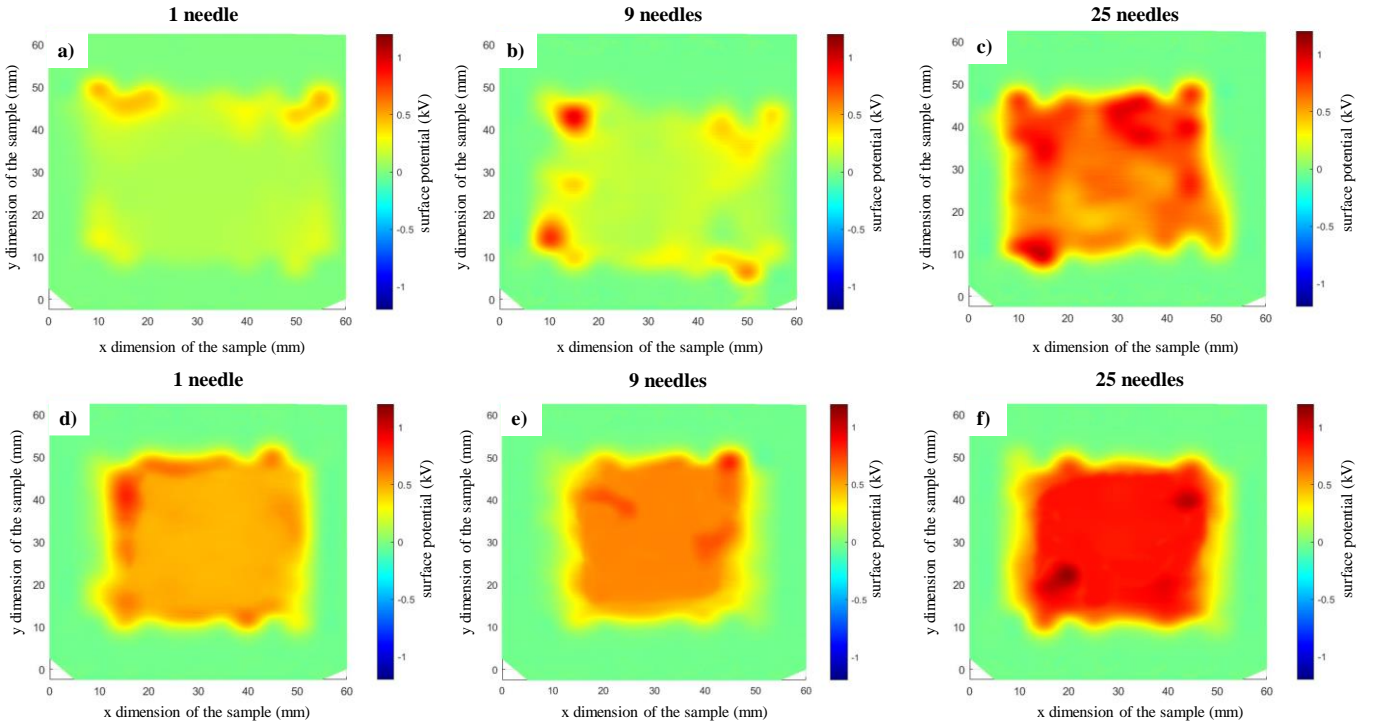


Fig. 4. Electrostatic potential maps for polarization without grid by using a) 1 needle, b) 9 needles and c) 25 needles. Electrostatic potential maps for polarization with grid by using d) 1 needle, e) 9 needles and f) 25 needles

needle. Similarly, in the corona triode process, three maps representing the electrostatic potential over the sample surface were obtained (Fig. 4 from d) to f)). An increase in the number of needles resulted in a higher deposition of surface charge on the specimen. Furthermore, a considerable influence of the presence or absence of the grid can be observed, particularly in the case of a single-needle process and in the test conducted with nine needles, which significantly affects the charge distribution. In particular, by comparing Fig. 4 a) and d), it is evident that the inclusion of the grid is sufficient to achieve a homogeneous surface potential over the whole specimen surface.

Additionally, in Table II were reported the mean and the standard deviation of the piezoelectric strain coefficient measured through electromechanical characterization. To evaluate the entire polarized surface, five tests were conducted on each sample to measure the  $d_{33}$  at different points. This approach allowed a complete evaluation of the  $d_{33}$  uniformity over the sample surface.

TABLE II  
PIEZOELECTRIC STRAIN COEFFICIENT OF THE SAMPLES

Gridless Configuration			
Specimen Number	1	2	3
$d_{33}$ (pC/N)	$-10.5 \pm 4.6$	$-12.8 \pm 3.0$	$-16.7 \pm 2.6$
Corona Triode Configuration			
Specimen Number	4	5	6
$d_{33}$ (pC/N)	$-15.2 \pm 1.2$	$-16.7 \pm 1.1$	$-17.5 \pm 0.6$

As expected, an increase in the number of needles employed leads to a corresponding increase in  $d_{33}$  (absolute value) for a given voltage applied to the needles. Furthermore, the presence of the grid not only increases the piezoelectric coefficient, but also reduces the standard deviation, resulting in a more uniform distribution of charges on the sample surface.

By comparing the results of  $d_{33}$  and the 2D maps obtained, it is evident that a low piezoelectric response, along with a high standard deviation, corresponds to maps with a minimal accumulated and unevenly distributed charge (Fig. 4 a), b)). In contrast, the presence of the grid enables the generation of maps characterized by relatively uniform surface potential values (Fig. 4 d), e) and f)), leading to high  $d_{33}$  values and low mean square deviation.

#### IV. CONCLUSIONS

Piezoelectric P(VDF-TrFE) 80/20 thin films were tested to evaluate the electromechanical response following the corona polarization process. In addition to the conventional electromechanical characterization technique involving the measurement of the piezoelectric strain coefficient  $d_{33}$ , an alternative approach was proposed, focusing on the evaluation of the surface potential of the polarized specimens. This technique involved the use of a non-contact probe placed at a distance of 3 mm from the specimen and connected to an electrostatic voltmeter to analyze the surface potential of the samples. The acquired data were recorded through an oscilloscope and subsequently processed to generate 2D

electrostatic maps. The results demonstrate a remarkable correlation between the generated 2D electrostatic maps and the measured  $d_{33}$  values on the surface of the samples. For instance, the use of 1 needle in the gridless corona polarization resulted in a  $d_{33}$  equal to  $-10.5$  pC/N with a standard deviation of  $4.6$  pC/N; whereas the corona triode polarization with 25 needles optimized both the  $d_{33}$  value ( $-17.5$  pC/N) and the standard deviation ( $0.6$  pC/N). This correspondence allows to confidently affirm that evaluating the surface potential provides a rapid and alternative method for assessing the impact of various parameters on the corona poling process.

#### REFERENCES

- [1] G. Selleri *et al.*, "Self-sensing composite material based on piezoelectric nanofibers," *Mater. Des.*, vol. 219, p. 110787, 2022, doi: 10.1016/j.matdes.2022.110787.
- [2] X. Wang, F. Sun, G. Yin, Y. Wang, B. Liu, and M. Dong, "Tactile-sensing based on flexible PVDF nanofibers via electrospinning: A review," *Sensors (Switzerland)*, vol. 18, no. 2, 2018, doi: 10.3390/s18020330.
- [3] G. Selleri *et al.*, "Energy harvesting and storage with ceramic piezoelectric transducers coupled with an ionic liquid-based supercapacitor," *J. Energy Storage*, vol. 60, no. December 2022, p. 106660, 2023, doi: 10.1016/j.est.2023.106660.
- [4] N. Sezer and M. Koç, "A comprehensive review on the state-of-the-art of piezoelectric energy harvesting," *Nano Energy*, vol. 80, no. October 2020, p. 105567, 2021, doi: 10.1016/j.nanoen.2020.105567.
- [5] G. Selleri *et al.*, "Study on the polarization process for piezoelectric nanofibrous layers," *Annu. Rep. - Conf. Electr. Insul. Dielectr. Phenomena, CEIDP*, vol. 2021-Decem, pp. 61–64, 2021, doi: 10.1109/CEIDP50766.2021.9705470.
- [6] G. Selleri, L. Gasperini, L. Piddiu, and D. Fabiani, "Comparison between AC and DC polarization methods of piezoelectric nanofibrous layers," in *2022 IEEE 4th International Conference on Dielectrics (ICD)*, Jul. 2022, pp. 90–93. doi: 10.1109/ICD53806.2022.9863546.
- [7] J. A. Giacometti and O. N. Oliveira, "Corona Charging of Polymers," *IEEE Trans. Electr. Insul.*, vol. 27, no. 5, pp. 924–943, 1992, doi: 10.1109/14.256470.
- [8] S. K. Mahadeva, J. Berring, K. Walus, and B. Stoeber, "Effect of poling time and grid voltage on phase transition and piezoelectricity of poly(vinylidene fluoride) thin films using corona poling," *J. Phys. D. Appl. Phys.*, vol. 46, no. 28, 2013, doi: 10.1088/0022-3727/46/28/285305.
- [9] C. X. J. Yi, Y. Song, S. Zhang, Z. Cao, C. Li, "Corona - Poled Porous Electrospun Films of Gram - Scale Y - Doped ZnO and PVDF Composites for Piezoelectric Nanogenerators," *Polymers (Basel)*, 2022.
- [10] M. S. Bendilmi, T. Zegloul, Z. Ziari, K. Medles, and L. Dascalescu, "Experimental Characterization of a Tri-Needle-Type Corona Electrode in View of Improving Charging Uniformity," *IEEE Trans. Ind. Appl.*, vol. 58, no. 1, pp. 783–791, 2022, doi: 10.1109/TIA.2021.3130012.
- [11] J. W. Zhang, Y. C. Cui, C. Putson, R. T. Liu, and C. L. Liu, "Surface charge accumulation effect of polyimide after temperature controlling corona polarization," *Proc. 2016 IEEE Int. Conf. Dielectr. ICD 2016*, vol. 2, pp. 1151–1154, 2016, doi: 10.1109/ICD.2016.7547821.
- [12] A. Cristofolini, G. Neretti, A. Popoli, A. C. Ricchiuto, and P. Seri, "Experimental and Numerical Investigation on the Electric Charge Deposition in a Dielectric Barrier Discharge," *Annu. Rep. - Conf. Electr. Insul. Dielectr. Phenomena, CEIDP*, vol. 2019-October, pp. 690–693, 2019, doi: 10.1109/CEIDP47102.2019.9009845.
- [13] L. Gasperini, G. Selleri, D. Pegoraro, and D. Fabiani, "Corona poling for polarization of nanofibrous mats advantages and open issues," *Annu. Rep. - Conf. Electr. Insul. Dielectr. Phenomena, CEIDP*, pp. 479–482, 2022.